Abnormal Superfluid Fraction of Harmonically Trapped Few-Fermion Systems

Yangqian Yan and D. Blume
Department of Physics and Astronomy, Washington State University, Pullman, Washington 99164-2814, USA
(Received 16 December 2013; revised manuscript received 7 February 2014; published 13 June 2014)

Superfluidity is a fascinating phenomenon that, at the macroscopic scale, leads to dissipationless flow and the emergence of vortices. While these macroscopic manifestations of superfluidity are well described by theories that have their origin in Landau's two-fluid model, our microscopic understanding of superfluidity is far from complete. Using analytical and numerical *ab initio* approaches, this Letter determines the superfluid fraction and local superfluid density of small harmonically trapped two-component Fermi gases as a function of the interaction strength and temperature. At low temperature, we find that the superfluid fraction is, in certain regions of the parameter space, negative. This counterintuitive finding is traced back to the symmetry of the system's ground state wave function, which gives rise to a diverging quantum moment of inertia I_q. Analogous abnormal behavior of I_q has been observed in even-odd nuclei at low temperature. Our predictions can be tested in modern cold atom experiments.

DOI: 10.1103/PhysRevLett.112.235301 PACS numbers: 67.85.Lm, 05.30.Fk, 34.50.−s, 67.85.−d

Superfluidity plays a crucial role in various areas of physics. The core of neutron stars is thought to be superfluid, giving rise to modifications of the specific heat and rapid cooling [1,2]. In laboratory settings, superfluidity of bosonic liquid helium-4 below 2.17 K and fermionic liquid helium-3 below 3 mK is associated with dissipationless flow and the formation of vortices [3]. More recently, superfluidity has been demonstrated in dilute atomic Bose and Fermi gas experiments [4–7]. The superfluid fraction shows a strong dependence on the dimensionality and the size of the system. In particular, transitions that are sharp in homogeneous systems are smeared out in finite-sized systems [8–10].

Over the past 20 years or so, nonclassical rotations in small doped bosonic helium-4 and molecular parahydrogen clusters have been interpreted within the framework of microscopic superfluidity [11–16]. This framework has been applied to systems consisting of as few as one, two, or three particles [17,18]. The framework of microscopic superfluidity dates back to the 1950s when nuclear physicists introduced a moment of inertia based method for the study of superfluidity in finite-sized nuclei [19–21]. In nuclei, superfluidity is tied to the pairing of nucleons [8,22,23]. As a consequence of pairing, the quantum moment of inertia of even-even nuclei, i.e., nuclei with an even number of protons and an even number of neutrons, tends to go to zero in the zero temperature limit while that of even-odd nuclei tends to increase sharply as the temperature approaches zero [8,23,24].

We investigate the superfluid fraction and local superfluid density of small harmonically trapped dilute atomic Fermi gases over a wide range of interaction strengths. In the low temperature region, we identify parameter combinations where the quantum moment of inertia is abnormally large, i.e., larger than the classical moment of inertia, implying a negative superfluid fraction. The negative superfluid fraction is linked to the topology of the density matrix. Specifically, the superfluid fraction takes on negative values in the low temperature regime when one of the energetically low-lying eigenstates supports a Pauli vortex with finite circulation [25–27] at the center of the trap. Intuitively, this can be understood as follows: In the absence of a low-energy eigenstate with finite circulation, the superfluid few-fermion gas "does not respond" to an infinitesimal rotation. This situation closely resembles that for a superfluid few-boson gas. In the presence of a low-energy eigenstate with finite circulation, however, the superfluid few-fermion gas "responds strongly" to an infinitesimal rotation; i.e., the infinitesimal rotation leads to a dynamical instability. A related instability also exists for bosonic few-atom systems. However, since the instability for bosons does not occur for an infinitesimal rotation but when the rotating frequency is comparable to the angular trapping frequency [28], the superfluid fraction, which is defined in the limit of infinitesimal rotation [29–32], is not affected by the instability. We note that a negative superfluid fraction has also been predicted to exist for the Fulde-Ferrell-Larkin-Ovchinnikov state of fermions loaded into an optical lattice [33]. The negative superfluid fraction discussed in this Letter is related to the occurrence of paramagnetism of polarized one-dimensional electrons on a ring with an even number of particles [34].

We consider N atoms of mass m described by the Hamiltonian H in a spherically symmetric harmonic trap. The system Hamiltonian under a small rotation about the z axis can, in the rotating frame, be expressed as $H_{\rm rot} = H - \Omega L_z$ [3], where Ω denotes the angular rotating frequency and L_z the z component of the angular momentum operator $\mathbf{L}$. The superfluid fraction n_s is defined as $n_s = 1 - I_q/I_c$ [29–32], where the quantum moment of inertia I_q

is defined in terms of the response to an infinitesimal rotation,

$$I_q = \frac{\partial \langle L_z \rangle_{\text{th}}}{\partial \Omega}\bigg|_{\Omega=0}, \tag{1}$$

and $\langle \cdot \rangle_{\text{th}}$ indicates the thermal average. The classical moment of inertia I_c is defined through $I_c = \langle m \sum_n r_{n,\perp}^2 \rangle_{\text{th}}$, where $r_{n,\perp}$ is the distance of the nth particle to the rotating axis [35].

We work in the canonical ensemble and determine the superfluid fraction of small trapped systems as a function of the temperature T using two different approaches. (i) We use the path integral Monte Carlo (PIMC) approach to sample the density matrix at temperature T [36–38]. The superfluid fraction n_s and local superfluid density ρ_s are then obtained using the area estimator [32,39,40]. (ii) We employ a microscopic approach [38]: For the systems considered, $\mathbf{L}^2$ and L_z commute with the Hamiltonian H, implying that the total orbital angular momentum quantum number L and corresponding projection quantum number M are good quantum numbers. One finds $I_q = \hbar^2 \langle M^2 \rangle_{\text{th}} / (k_B T)$, where the thermal average runs over the system at rest [41]. To evaluate I_q, we calculate a large portion of the quantum mechanical energy spectrum and thermally average the quantity M^2. From the same set of calculations we determine $r_{n,\perp}^2$ (and correspondingly I_c) via the generalized virial theorem [42–44], which applies to systems with short-range interactions with s-wave scattering length a_s under spherically symmetric harmonic confinement with angular trapping frequency ω, $3\omega^2 \sum_n \langle m r_{n,\perp}^2 \rangle_{\text{th}} = 2\langle E + a_s(\partial E/\partial a_s)/2 \rangle_{\text{th}}$. Here, E denotes the total energy.

We first consider N identical noninteracting harmonically trapped bosons or fermions described by the Hamiltonian $H = H_{\text{ni}}$,

$$H_{\text{ni}} = \sum_{j=1}^{N} \left(\frac{-\hbar^2}{2m} \nabla_j^2 + \frac{1}{2} m \omega^2 \mathbf{r}_j^2 \right), \tag{2}$$

where $\mathbf{r}_j$ denotes the position vector of the jth atom. Using the N-body partition function, we calculate the thermal averages for I_c and I_q [45]. Figure 1(b) shows n_s for $N = 1$–10 noninteracting bosons. For all N, n_s goes to 1 as the temperature approaches zero. This is a direct consequence of the fact that the ground state has $L = 0$. As the particle number increases, the superfluid region broadens. Figure 1(a) shows n_s for $N = 1$–10 noninteracting fermions. The curves have similar asymptotic behavior at high temperature, yet differ dramatically at low temperature. The $N = 1, 4$, and 10 curves increase monotonically with decreasing temperature and approach one at $T = 0$. Because of the closed shell nature, the ground state of these Fermi systems is, as that of the Bose systems, nondegenerate and has vanishing angular momentum. The curves for

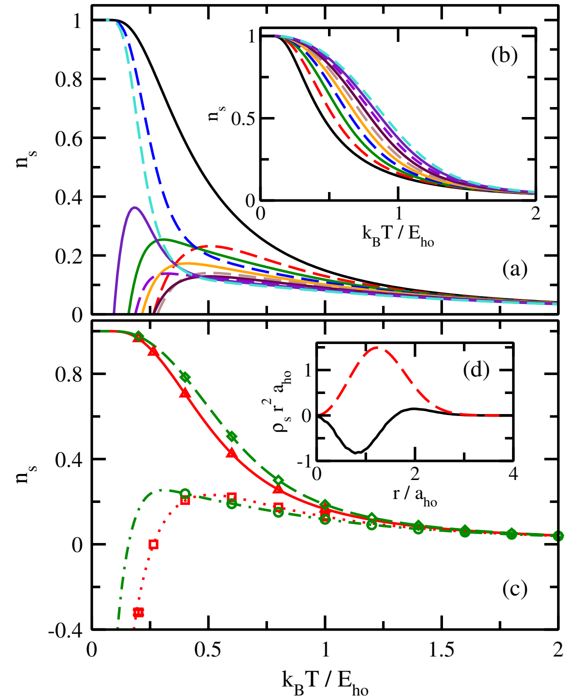

FIG. 1 (color online). Superfluid properties of the noninteracting trapped single-component gas as a function of $k_B T / E_{\text{ho}}$. (a) From top to bottom at $k_B T = E_{\text{ho}}$, the alternating solid and dashed lines show n_s for the Fermi gas with $N = 1$–10. (b) From bottom to top, alternating solid and dashed lines show n_s for the Bose gas with $N = 1$–10. (c) The dashed and solid lines replot n_s for $N = 2$ and 3, respectively. For comparison, symbols show n_s obtained using the PIMC approach. The error bars are smaller than the symbol size. (d) The dashed and solid lines show the scaled radial total and superfluid density for $N = 2$.

the other N values dive down to negative infinity at zero temperature. The ground state of these open-shell systems is degenerate and contains finite angular momentum states. Figure 1(c) compares the analytical results (lines) for $N = 2$ and 3 with those obtained by the PIMC approach (symbols). The excellent agreement confirms the correctness of our analytical results and demonstrates that our PIMC simulations yield highly accurate results. Given that BCS theory predicts a vanishing superfluid fraction for the homogeneous Fermi gas in the absence of an effective attraction, one might wonder where the nonvanishing n_s values for the noninteracting trapped Fermi gas come from. Our analysis shows that the nonvanishing n_s is due to the trap energy scale E_{ho}, where $E_{\text{ho}} = \hbar\omega$. An analogous energy scale does not exist in the noninteracting homogeneous system, for which the moment of inertia based method predicts, in agreement with BCS theory, that n_s vanishes. Last, we note that although Stringari [48] determined n_s for trapped noninteracting single-component Fermi gases, no negative superfluid fraction was observed because the semiclassical treatment employed assumed $k_B T \gg E_{\text{ho}}$.

To get a sense of the spatial distribution of the superfluid fraction, we calculate the radial superfluid density $\rho_s(r)$. Our analysis is based on the definitions of Refs. [40,49]; we note that alternative definitions exist [50–52]. As an example, the solid line in Fig. 1(d) shows the scaled radial superfluid density $\rho_s(r)r^2$ for the two-fermion system at $T = 0.265E_{\rm ho}/k_B$. For comparison, the dashed line shows the scaled radial total density at the same temperature. For this temperature, we have $n_s = 0$ [53]. The radial superfluid density is negative for small r and positive for large r. In the absence of rotation, the ground state has $L = 1$ and the expectation value of L_z averages to zero. The threefold degenerate state splits under a small rotation, with the $M = 1$ state having the lowest energy; correspondingly, the expectation value of L_z is $\hbar$. Using these results to express I_q, see Eq. (1), as a finite difference, we find that I_q scales as $\lim_{\Omega\to 0}\hbar\Omega^{-1}$ at $T = 0$. This shows that the divergence of I_q (and, hence, the negative value of n_s) is due to the $M = 1$ state, which contains a vortex at the center of the trap with circulation 1. Figure 1(d) shows that this is where the radial superfluid density is negative; i.e., the admixture of the vortex state triggers the dynamical instability.

Next, we consider two-component Fermi gases consisting of N_1 spin-up and $N - N_1$ spin-down particles with short-range interspecies interactions. As the s-wave scattering length is tuned from small negative values to infinity to small positive values, the system changes from forming Cooper pairs to composite bosonic molecules [54]. In what follows we investigate how the change from “fermionic” (Cooper pairs) to “bosonic” (composite molecules) is reflected in the superfluid properties of the trapped system. We consider the Hamiltonian $H = H_{\rm int}$,

$$H_{\rm int} = H_{\rm ni} + \sum_{j=1}^{N_1} \sum_{k=N_1+1}^{N} V_{\rm tb}(\mathbf{r}_{jk}), \tag{3}$$

for two different interspecies two-body potentials $V_{\rm tb}$, a regularized zero-range pseudopotential V_F [55] and a short-range Gaussian potential V_G with depth U_0 ($U_0 < 0$) and range r_0, $V_G(\mathbf{r}_{jk}) = U_0 \exp[-\mathbf{r}_{jk}^2/(2r_0^2)]$. The depth and range are adjusted so that V_G yields the desired a_s; throughout, we consider potentials with $r_0 \ll a_{\rm ho}$ [$a_{\rm ho} = \sqrt{\hbar/(m\omega)}$] that support at most one free-space s-wave bound state.

For the trapped (2,1) system with zero-range interactions, we determine a large portion of the energy spectrum by solving the Lippman Schwinger equation for arbitrary scattering length [56]. This means that n_s can be determined within the microscopic approach over a wide temperature regime. Figure 2(b) shows the classical moment of inertia I_c of the (2,1) system as a function of the temperature for different $1/a_s$ (a_s positive). I_c decreases for fixed T with increasing $1/a_s$ and increases for fixed a_s with increasing T. Figure 2(c) shows the quantum moment of

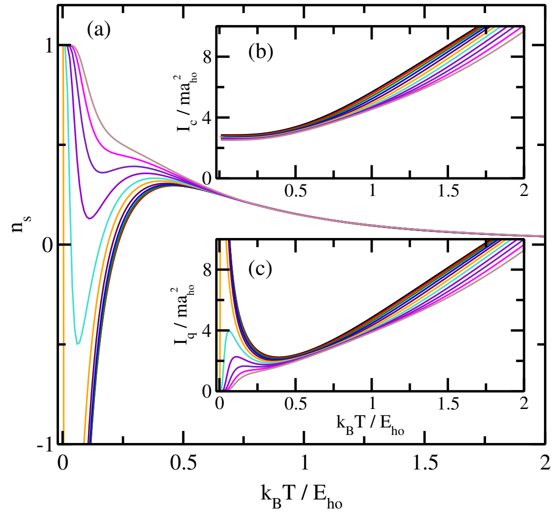

FIG. 2 (color online). Properties of the interacting trapped (2,1) system as a function of $k_BT/E_{\rm ho}$. (a) The lines from bottom to top show n_s for $a_{\rm ho}/a_s = 0, 0.2, \ldots, 2$. (b),(c) The lines from top to bottom show I_c and I_q, respectively, for $a_{\rm ho}/a_s = 0, 0.2, \ldots, 2$.

inertia I_q. In the high temperature regime, I_q and I_c are nearly identical. However, in the low temperature regime, notable differences exist. For $1/a_s = 0$, I_q diverges to positive infinity as $T \to 0$. For $a_{\rm ho}/a_s \approx 1$, in contrast, I_q is zero at $T = 0$, increases sharply for $k_BT \lesssim 0.1E_{\rm ho}$, and then decreases for $k_BT \approx 0.1$–$0.5E_{\rm ho}$. As $a_{\rm ho}/a_s$ increases, the local maximum moves to larger temperatures and eventually disappears for $a_{\rm ho}/a_s \approx 2$. The dramatic change of I_q at low T on the positive a_s side can be traced back to the symmetry change of the ground state wave function. The lowest eigenstate of the (2,1) system has $L = 1$ for $a_{\rm ho}/a_s \lesssim 1$ and $L = 0$ for $a_{\rm ho}/a_s \gtrsim 1$. Correspondingly, I_q goes, in the zero T limit, to $+\infty$ for $a_{\rm ho}/a_s \lesssim 1$ and to 0 for $a_{\rm ho}/a_s \gtrsim 1$. The strong variation of I_q near $a_{\rm ho}/a_s \approx 1$ in the low T regime reflects the “competing” contributions of the $L = 0$ and $L = 1$ states to the thermal average.

Combining I_c and I_q yields n_s [see Fig. 2(a)]. The (2,1) systems with $a_{\rm ho}/a_s \lesssim 1$ and $a_{\rm ho}/a_s \gtrsim 1$ have a superfluid fraction that goes to negative infinity and one, respectively, at zero temperature. This can be viewed as a “quantum phase transitionlike” feature [56,57]. At $k_BT = 0.2E_{\rm ho}$—a temperature that might be achievable with current experimental setups [58,59]—n_s varies between $-0.14(1)$ and $0.54(1)$ for $a_{\rm ho}/a_s = 0$ to 2. For a given a_s, n_s varies notably over a small temperature regime. The fact that n_s is essentially independent of a_s for $k_BT \gtrsim 0.75E_{\rm ho}$ and strongly dependent on a_s for $k_BT \lesssim 0.4E_{\rm ho}$ might prove advantageous for qualitatively verifying the predicted behavior experimentally.

We now investigate a trapped spin-balanced system. Figure 3(a) shows n_s for the (2,2) system with $a_s/a_{\rm ho} = 0, -0.2, -1$, and ∞. The ground state of the noninteracting (2,2) system is ninefold degenerate (one state has $L = 0$,

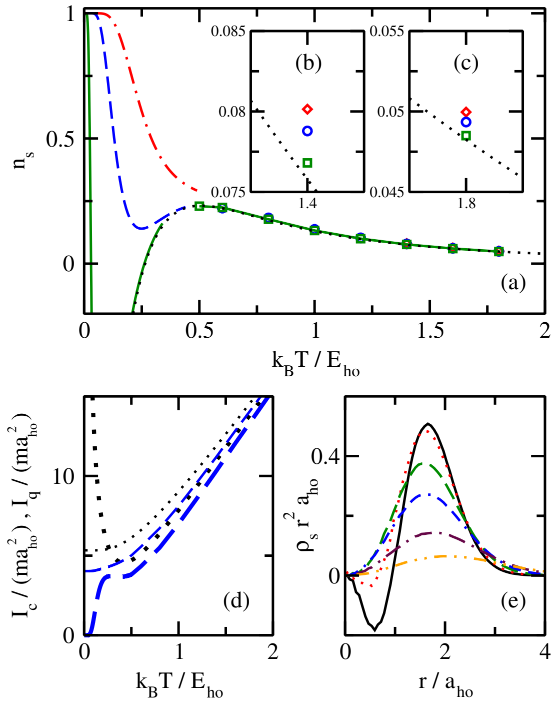

FIG. 3 (color online). Properties of the trapped (2,2) system. (a) The dotted, solid, dashed, and dash-dotted lines show n_s as a function of k_BT/E_{ho} for $a_s/a_{\mathrm{ho}} = 0, -0.2, -1$, and ∞, respectively. The squares, circles, and diamonds show n_s obtained by the PIMC approach for $a_s/a_{\mathrm{ho}} = -0.2, -1$, and ∞, respectively. (b) and (c) show blowups of the high-temperature region. (d) The thin dotted and dashed lines show I_c for $a_s = 0$ and $-a_{\mathrm{ho}}$, respectively; the thick dotted and dashed lines show I_q for $a_s = 0$ and $-a_{\mathrm{ho}}$, respectively. The dashed curves are obtained by the microscopic approach (using $r_0 = 0.06a_{\mathrm{ho}}$) for $k_BT/E_{\mathrm{ho}} \leq 0.5$ and by the PIMC approach (using $r_0 = 0.1a_{\mathrm{ho}}$) for $k_BT/E_{\mathrm{ho}} \geq 0.6$. (e) The solid, dotted, dashed, dash-dash-dotted, dash-dotted, and dash-dot-dotted lines show $\rho_s r^2$ for $a_s = -0.2a_{\mathrm{ho}}$ and $k_BT/E_{\mathrm{ho}} = 0.5, 0.6, 0.8, 1, 1.4$, and 2, respectively.

three states have $L = 1$, and five states have $L = 2$). The degeneracy of the ground state makes I_q [see thick dotted line in Fig. 3(d)] diverge to plus infinity at $T = 0$. The superfluid fraction, in turn, goes to minus infinity as $T \to 0$. As the interactions are turned on, the degeneracy of the states with different L is lifted, with the energy of the $L = 0$ state lying below that of the $L = 1$ and 2 states. This implies that I_q goes to zero at $T = 0$ for $a_s \neq 0$ [for $a_s/a_{\mathrm{ho}} = -1$, see the thick dashed line in Fig. 3(d)]. The behavior of the (2,2) system is similar to that of the (2,1) system in that the zero temperature limit of n_s changes from minus infinity to one as the scattering length is tuned. The transition, however, occurs at different scattering lengths [$a_s = 0$ for the (2,2) system and $a_{\mathrm{ho}}/a_s \approx 1$ for the (2,1) system].

Figure 3(e) shows the radial superfluid density for the (2,2) system with $a_s = -0.2a_{\mathrm{ho}}$ for various temperatures. For the lowest temperature considered ($k_BT = 0.5E_{\mathrm{ho}}$), n_s is equal to 0.230(3). Although n_s is positive, the radial superfluid density is negative in the small r region, reflecting the admixture of finite L states to the density matrix. As the temperature increases, the amplitude of the negative part of the radial superfluid density decreases and moves to smaller r. When the radial superfluid density is positive everywhere, it roughly has the same shape as the total radial density (not shown) but with significantly decreased amplitude. This shows that the superfluid density is, in this regime, distributed roughly uniformly throughout the cloud and not localized primarily near the center or edge of the cloud. We find similar behavior for other a_s.

In practice, thermal equilibrium cannot be reached if the confinement is spherically symmetric. We have checked that our results hold qualitatively for anisotropic traps provided that $|\omega_x - \omega_y| \ll \omega_x + \omega_y$. Moreover, the abnormal behavior of n_s and I_q is also found for finite rotating frequencies, provided that $\hbar\Omega \ll E_{\mathrm{ho}}$. Instead of probing the response to a rotation of the trap, it might be possible to simulate the rotation (and the resulting effective magnetic field) by applying an effective gauge field [60].

To summarize, we determined the superfluid properties of small harmonically trapped Fermi gases as functions of the s-wave scattering length and temperature. At low temperature, the quantum moment of inertia behaves, in certain regimes, abnormal; i.e., it is larger than the classical moment of inertia, yielding a negative superfluid fraction. The abnormal behavior arises if one or more of the low-lying eigenstates have a finite circulation, i.e., support a vortex. The relevant temperature is roughly $\lesssim 0.5E_{\mathrm{ho}}/k_B$. Our predictions are unique to small systems, since such low temperatures can only be reached in few-fermion systems [58,59] and not in large Fermi gases.

Support by the National Science Foundation (NSF) through Grant No. PHY-1205443 is gratefully acknowledged. This work used the Extreme Science and Engineering Discovery Environment (XSEDE), which is supported by NSF Grant No. OCI-1053575, and the WSU HPC.

[1] D. Page, M. Prakash, J. M. Lattimer, and A. W. Steiner, Phys. Rev. Lett. **85**, 2048 (2000).
[2] D. Page, M. Prakash, J. M. Lattimer, and A. W. Steiner, Phys. Rev. Lett. **106**, 081101 (2011).
[3] D. R. Tilley and J. Tilley, *Superfluidity and Superconductivity* (Institute of Physics Publishing, Philadelphia, 1990), 3rd ed.
[4] M. R. Matthews, B. P. Anderson, P. C. Haljan, D. S. Hall, C. E. Wieman, and E. A. Cornell, Phys. Rev. Lett. **83**, 2498 (1999).
[5] K. W. Madison, F. Chevy, W. Wohlleben, and J. Dalibard, Phys. Rev. Lett. **84**, 806 (2000).
[6] J. R. Abo-Shaeer, C. Raman, J. M. Vogels, and W. Ketterle, Science **292**, 476 (2001).
[7] M. W. Zwierlein, J. R. Abo-Shaeer, A. Schirotzek, C. H. Schunck, and W. Ketterle, Nature (London) **435**, 1047 (2005).

[8] P. Ring and P. Schuck, *The Nuclear Many-Body Problem* (Springer-Verlag, New York, 1980).
[9] L. Pitaevskii and S. Stringari, *Bose-Einstein Condensation* (Oxford University Press, New York, 2003).
[10] C. J. Pethick and H. Smith, *Bose-Einstein Condensation in Dillute Gases* (Cambridge University Press, Cambridge, England, 2008), 2nd ed.
[11] J. P. Toennies and A. F. Vilesov, Angew. Chem., Int. Ed. Engl. **43**, 2622 (2004).
[12] S. Grebenev, J. P. Toennies, and A. F. Vilesov, Science **279**, 2083 (1998).
[13] S. Grebenev, B. Sartakov, J. P. Toennies, and A. F. Vilesov, Science **289**, 1532 (2000).
[14] J. Tang, Y. Xu, A. R. W. McKellar, and W. Jäger, Science **297**, 2030 (2002).
[15] Y. Kwon and K. B. Whaley, Phys. Rev. Lett. **89**, 273401 (2002).
[16] F. Paesani, Y. Kwon, and K. B. Whaley, Phys. Rev. Lett. **94**, 153401 (2005).
[17] See, e.g., S. A. Khairallah, M. B. Sevryuk, D. M. Ceperley, and J. P. Toennies, Phys. Rev. Lett. **98**, 183401 (2007) and P. L. Raston, W. Jäger, H. Li, R. J. Le Roy, and P.-N. Roy, Phys. Rev. Lett. **108**, 253402 (2012).
[18] We stress that the superfluid fraction is a well-defined quantity for large and small systems.
[19] A. Bohr, B. R. Mottelson, and D. Pines, Phys. Rev. **110**, 936 (1958).
[20] S. T. Belyaev, K. Dan. Vidensk. Selsk. Mat. Fys. Medd. **31**, No. 11, 1 (1959).
[21] A. Migdal, Nucl. Phys. **13**, 655 (1959).
[22] D. J. Dean and M. Hjorth-Jensen, Rev. Mod. Phys. **75**, 607 (2003).
[23] R. A. Broglia and V. Zelevinsky, *Fifty Years of Nuclear BCS: Pairing in Finite Systems* (World Scientific, Singapore, 2013).
[24] Y. Alhassid, G. F. Bertsch, L. Fang, and S. Liu, Phys. Rev. C **72**, 064326 (2005).
[25] H. Saarikoski, S. M. Reimann, A. Harju, and M. Manninen, Rev. Mod. Phys. **82**, 2785 (2010).
[26] P. A. Dirac, Proc. R. Soc. A **133**, 60 (1931).
[27] J. O. Hirschfelder, C. J. Goebel, and L. W. Bruch, J. Chem. Phys. **61**, 5456 (1974).
[28] D. Dagnino, N. Barberán, M. Lewenstein, and J. Dalibard, Nat. Phys. **5**, 431 (2009).
[29] A. J. Leggett, Phys. Rev. Lett. **25**, 1543 (1970).
[30] G. Baym, in *Mathematical Methods in Solid State and Superfluid Theory*, edited by R. Clark and E. Derrick (Oliver and Boyd, Edinburgh, 1969).
[31] A. J. Leggett, Phys. Fenn. **8**, 125 (1973).
[32] E. L. Pollock and D. M. Ceperley, Phys. Rev. B **36**, 8343 (1987).
[33] T. Paananen, J. Phys. B **42**, 165304 (2009).
[34] X. Waintal, G. Fleury, K. Kazymyrenko, M. Houzet, P. Schmitteckert, and D. Weinmann, Phys. Rev. Lett. **101**, 106804 (2008).
[35] The distance $r_{n,\perp}$ between $\vec{r}_n$ and the axis $\hat{z}$ can be expressed as $r_{n,\perp} = |\vec{r}_n \times \hat{z}|$.
[36] D. M. Ceperley, Rev. Mod. Phys. **67**, 279 (1995).
[37] M. Boninsegni, J. Low Temp. Phys. **141**, 27 (2005).
[38] Y. Yan and D. Blume, Phys. Rev. A **88**, 023616 (2013).
[39] P. Sindzingre, M. L. Klein, and D. M. Ceperley, Phys. Rev. Lett. **63**, 1601 (1989).
[40] Y. Kwon, F. Paesani, and K. B. Whaley, Phys. Rev. B **74**, 174522 (2006).
[41] J. M. Blatt and S. T. Butler, Phys. Rev. **100**, 476 (1955).
[42] S. Tan, Ann. Phys. (N.Y.) **323**, 2987 (2008).
[43] S. Tan, Ann. Phys. (N.Y.) **323**, 2971 (2008).
[44] S. Tan, Ann. Phys. (N.Y.) **323**, 2952 (2008).
[45] The partition function of the noninteracting N-particle system can be obtained by symmetrizing (antisymmetrizing) the single-particle partition function for bosons (fermions) [46]. By the virial theorem [47], I_c is equal to $2\langle E\rangle_{\mathrm{th}}/(3\omega^2)$. To calculate I_q, we note that $\langle M^2\rangle_{\mathrm{th}} = \langle(\sum_n M_n)^2\rangle_{\mathrm{th}}$ simplifies to $\langle\sum_n M_n^2\rangle_{\mathrm{th}}$ since the cross terms cancel; here, M_n is the projection quantum number of the nth particle.
[46] W. Krauth, *Statistical Mechanics: Algorithms and Computations*, Oxford Master Series in Physics (Oxford University Press, Oxford, 2006). The permutations of the N-particle system are realized using the function IntegerPartitions in *Mathematica*.
[47] W. Greiner, *Quantum Mechanics: An Introduction* (Springer-Verlag, Berlin, 2001), 4th ed. The virial theorem is a special case of the generalized virial theorem with $a_s = 0$.
[48] S. Stringari, Phys. Rev. Lett. **76**, 1405 (1996).
[49] $\rho_s(\mathbf{r})$ satisfies $I_c - I_q = m\int\rho_s(\mathbf{r})r_\perp^2 d^3\mathbf{r}$, where $r_\perp$ denotes the distance to the z axis.
[50] A. B. Pippard, Proc. R. Soc. A **216**, 547 (1953).
[51] Y. Kwon and K. B. Whaley, Phys. Rev. Lett. **83**, 4108 (1999).
[52] E. W. Draeger and D. M. Ceperley, Phys. Rev. Lett. **90**, 065301 (2003).
[53] The "direct" integral $4\pi\int_0^\infty \rho_s(r)r^2 dr$, i.e., the area under the curve, is not zero since the radial superfluid density needs to be multiplied by an "extra" $r_\perp^2$ factor to yield the moment of inertia [40].
[54] S. Giorgini, L. P. Pitaevskii, and S. Stringari, Rev. Mod. Phys. **80**, 1215 (2008).
[55] K. Huang and C. N. Yang, Phys. Rev. **105**, 767 (1957).
[56] J. P. Kestner and L.-M. Duan, Phys. Rev. A **76**, 033611 (2007).
[57] P. O. Bugnion, J. A. Lofthouse, and G. J. Conduit, Phys. Rev. Lett. **111**, 045301 (2013).
[58] F. Serwane, G. Zürn, T. Lompe, T. B. Ottenstein, A. N. Wenz, and S. Jochim, Science **332**, 336 (2011).
[59] A. N. Wenz, G. Zürn, S. Murmann, I. Brouzos, T. Lompe, and S. Jochim, Science **342**, 457 (2013).
[60] N. R. Cooper and Z. Hadzibabic, Phys. Rev. Lett. **104**, 030401 (2010).